Tightening energetic bounds on linear gyrokinetic instabilities

Paul Costello and **Gabriel Plunk**

Max-Planck-Institut für Plasmaphysik, Wendelsteinstraße 1, 17491 Greifswald, Germany
Corresponding author: Paul Costello, paul.costello@ipp.mpg.de

Bounding energetic growth of gyrokinetic instabilities is a complementary approach to linear instability analyses involving normal eigenmodes. Previous work has focused on upper bounds which are valid linearly and nonlinearly. However, if an upper bound on linear instability growth is desired, these nonlinearly valid bounds may be a poor predictor of the growth of the most unstable eigenmode. This is most evident for the simplest of instabilities: the ion-temperature-gradient (ITG) mode in a slab geometry. In this work, we derive energetic upper bounds specifically for linear instability growth, focusing on the slab ITG. We show that there is no fundamental limitation on how tightly linear growth can be bounded by an energetic norm, with the tightest possible bound being given by a special energy comprising projection coefficients of the linear eigenmode basis. Additionally, we consider 'constrained optimal modes' that maximise energy growth subject to constraints that are also obeyed by the linear eigenmodes. This yields computationally efficient upper bounds that closely resemble the linear growth rate, capturing effects connected to the real frequency of instabilities, which have been absent in the energetic bounds considered thus far.

Key words: plasma instabilities, fusion plasma

---

1. Introduction

Most studies of gyrokinetic microinstabilities are concerned with linear eigenmodes of the gyrokinetic equation, solutions that evolve in time as $\exp(-i\omega t)$, where $\omega = \omega_r + i\gamma$ is a complex frequency. If $\gamma > 0$, these modes grow exponentially as $t \to \infty$ in the absence of any nonlinear interaction. The linear eigenmodes of the gyrokinetic equation are famously diverse and contribute to the richness of gyrokinetic theory but also complicate the computation of instability growth rates. For instance, it can be difficult to distinguish modes of different types (Kammerer, Merz & Jenko 2008), which react differently to changing plasma parameters. Recently, a new approach for studying microinstabilities has been developed in a series of papers (Helander & Plunk 2021, 2022; Plunk & Helander 2023), in which instability growth is instead bounded from above by the growth of optimal modes. These modes are distinct from linear eigenmodes and are derived by choosing an energetic quadratic

norm of the gyrokinetic system, say E, and seeking the distribution functions that maximise the normalised instantaneous growth of this energy, $\Lambda = (2E)^{-1} \mathrm{d}E/\mathrm{d}t$. The growth of the fastest growing optimal mode, $\Lambda_{\max}$, provides an upper bound on the allowable instantaneous growth of the system, and if the energetic norm considered is chosen carefully (such that it is invariant over the sum of nonlinear interactions) this bounds the growth of the linear system at each scale and bounds the nonlinear growth of the system when all scales are accounted for. The growth of the most unstable linear eigenmode at each scale necessarily satisfies

$$\gamma \leqslant \Lambda_{\max}. \tag{1.1}$$

Although turbulence is a fundamentally nonlinear phenomenon, linear eigenmode analyses is often an informative endeavour, perhaps more than one would expect. This is evidenced by extensive gyrokinetic simulation work (Dannert & Jenko 2005; Pueschel *et al.* 2016; Hatch *et al.* 2011, 2016) that shows that linear eigenmodes often survive nonlinearly. This observation forms the basis for quasilinear theory, which has proven to be a useful tool in modelling turbulent transport (Bourdelle *et al.* 2007; Giacomin *et al.* 2025).

Until now, the gyrokinetic optimal modes have been computed with both linear and nonlinear growth in mind, often leading to large differences when the upper bound is compared with linear growth rates (Podavini *et al.* 2025). This is most evident for the classic case of instability driven by an ion-temperature gradient (ITG) in a uniform magnetic field (i.e. the slab ITG mode), for which Plunk & Helander (2023) found that even a resonance-informed upper bound exhibited vastly different qualitative behaviour to the linear growth rate at small values of the temperature gradient. In this work, we explore ways to specialise the optimal mode analysis for the purpose of bounding linear instability growth, focusing specifically on the slab ITG mode, which exemplifies the shortcomings of the upper bounds considered thus far for the purpose of bounding linear instabilities.

Our work consists of two main parts. Firstly, we pose the question 'how tightly can linear eigenmode growth be bounded by optimal modes' and find that the optimal mode growth spectrum can be made to correspond exactly to the growth rate spectrum of linear eigenmodes, giving a one-to-one correspondence between linear eigenmodes and optimal modes for this special energetic norm, which we refer to as the Case–Van Kampen energy.

With this theoretical result underfoot, we then seek simpler upper bounds on linear instability growth by considering what we refer to as constrained optimal modes. This approach results in a low-dimensional, linear system of gyrofluid-like moment equations. The growth of these constrained optimal modes exhibits a dependence on key instability parameters that is qualitatively very similar to the linear eigenmodes in the slab ITG case, even exhibiting a critical gradient which arises due to resonant stabilisation, despite the low-dimensionality of the system. Unlike traditional gyrofluid theories, which often involve an *ad hoc* closure to capture these effects, the constrained optimal modes make no such approximation, providing a rigorous bound on fully kinetic linear instability growth.

2. Linear gyrokinetic equation

Here, we concern ourselves with the electrostatic limit of the gyrokinetic equation in a flux tube geometry, where the fluctuations are periodic in the directions perpendicular to the magnetic field, which is given by $\boldsymbol{B} = \nabla\psi \cdot \nabla\alpha$. In these coordinates, ψ acts as a 'radial' coordinate (in the sense that the plasma gradients will be in the

coordinate ψ), and α is binormal to the magnetic field and the gradient direction. The coordinate along the magnetic field lines is denoted by l. Because we wish to test the limits of the optimal modes' ability to bound the growth of linear instabilities, we must consider a scenario where the linear eigenmodes are well understood.[1] To this end, we consider the case of a uniform magnetic geometry (henceforth called the 'slab' geometry), in which a single Fourier mode along the magnetic field line can be considered, such that $\partial/\partial l \to i k_\parallel$.

Moreover, we consider only a single kinetic species, focusing on the familiar limit of kinetic ions with adiabatic electrons (Kadomtsev & Pogutse 1970; Biglari, Diamond & Rosenbluth 1989; Plunk *et al*. 2014). In this scenario, the gyrokinetic equation becomes

$$\frac{\partial g}{\partial t} + i v_\parallel k_\parallel g = \frac{e F_0}{T_i} \left(\frac{\partial}{\partial t} + i \omega_*^T \right) \phi J_0. \tag{2.1}$$

Here, $g = g(\mu, E, \boldsymbol{k}_\perp, k_\parallel)$ is the (Fourier transformed) non-adiabatic part of the perturbed ion distribution function. The phase space variables are the particle energy $E = m v^2/2$ and the magnetic moment $\mu = m v_\perp^2/(2B)$, where $v^2 = v_\perp^2 + v_\parallel^2$, $m = m_i$ is the ion mass, $v_\perp$ and $v_\parallel$ are the components of the particle velocity in the plane perpendicular to, and parallel to $\boldsymbol{B}$, respectively. The ions are assumed to have a Maxwellian background distribution $F_0 = n(\psi)/(v_T^3 \pi^{3/2}) \exp(-v^2/v_T^2)$ with a number density $n(\psi)$, where the ion temperature T_i enters via the thermal speed $v_T = \sqrt{2 T_i/m}$ and $T_i = T_i(\psi)$. The plasma gradients enter via the energy-dependent diamagnetic frequency $\omega_*^T = \omega_*(1 + \eta[v^2/v_T^2 - 3/2])$ where $\omega_* = (k_\alpha T_i/e)(\mathrm{d}\ln n/\mathrm{d}\psi)$ and $\eta = \mathrm{d}\ln T_i/\mathrm{d}\ln n$, with e the ion charge. The Bessel function of the first kind J_0, which arises due to the gyro-average, has the argument $J_0 = J_0(k_\perp v_\perp/\Omega)$ where $\Omega = e B/m$. The system is closed by quasi-neutrality

$$\frac{e^2 n}{T_i}(1 + \tau)\phi = e \int_{-\infty}^{\infty} \mathrm{d}v_\parallel \int_0^{\infty} \mathrm{d}v_\perp v_\perp 2\pi g J_0 = e \int_{-\infty}^{\infty} \bar{g} \, \mathrm{d}v_\parallel, \tag{2.2}$$

where ϕ is the Fourier transformed electrostatic potential and τ is the ion–electron temperature ratio $\tau = T_i/T_e$. Additionally, we have defined the reduced distribution function $\bar{g}(v_\parallel) = 2\pi \int_0^{\infty} v_\perp g J_0 \mathrm{d}v_\perp$.

Because the wave–particle resonance is one-dimensional in phase space in a slab geometry, we may integrate (2.1) over $v_\perp$ to express the gyrokinetic equation in terms of $\bar{g}$. This yields

$$\frac{\partial \bar{g}}{\partial t} + i v_\parallel k_\parallel \bar{g} = \frac{e \bar{F}_0}{T_i} \left[G_{\perp 0} \left(\frac{\partial}{\partial t} + i \omega_*(1 + \eta(x_\parallel^2 - 3/2)) \right) + i \omega_* \eta G_{\perp 2} \right] \phi, \tag{2.3}$$

where $\bar{F}_0 = n/(v_T \sqrt{\pi}) e^{-v_\parallel^2/v_T^2}$ and $x_\parallel = v_\parallel/v_T$. The functions $G_{\perp 0}$ and $G_{\perp 2}$ can be written in terms of the familiar $\Gamma_n(b) = I_n(b)e^{-b}$ functions of gyrokinetic theory where I_n is a modified Bessel function and $b = k_\perp^2 \rho^2$ with $\rho = v_T/(\Omega\sqrt{2})$ (see Plunk & Helander (2023) for specifics)

$$G_{\perp 0}(b) = \Gamma_0(b), \tag{2.4}$$

$$G_{\perp 2}(b) = \Gamma_0(b) - b[\Gamma_0(b) - \Gamma_1(b)]. \tag{2.5}$$

---

[1]In fact, as we will see later, we actually require complete knowledge of the infinite set of linear modes to achieve our tightest bound on linear growth.

The linear eigenmodes of (2.3) have been well studied (Kadomtsev & Pogutse 1970; Plunk *et al*. 2014) allowing clear comparison between the linear growth rates and the bounds derived here.

3. Tightest possible energetic bounds

Before attempting to tailor the optimal mode analysis to bounding the growth of linear instabilities, we will determine whether there is a fundamental limitation of the optimal modes when it comes to bounding linear eigenmode growth. In other words, how tightly can the growth of the linear modes be bounded by the instantaneous growth of an energetic norm? To answer this question, we will leverage techniques that are seldom used in gyrokinetics (Heninger & Morrison 2018; Plunk 2013, 2015). We begin by defining $f = \bar{g} - e\bar{F}_0 G_{\perp 0}\phi/T_i$, allowing us to write (2.3) as

$$\frac{\partial f}{\partial t} + i v_\parallel k_\parallel f = -i k_\parallel S(v_\parallel, k_\parallel, b) \int f(v'_\parallel)\mathrm{d}v'_\parallel, \tag{3.1}$$

where we have used quasi-neutrality to close the system in terms of an intergo-differential equation and defined

$$S(v_\parallel) = \frac{\bar{F}_0}{n(1 + \tau - G_{\perp 0})}\left[v_\parallel G_{\perp 0} - \frac{\omega_*}{k_\parallel}\left(G_{\perp 0}(1 + \eta(x_\parallel^2 - 3/2)) + \eta\, G_{\perp 2}\right)\right], \tag{3.2}$$

where we have suppressed the dependence on other parameters e.g. $k_\parallel$ and $k_\perp$. Equation (3.1) is equivalent to the linear system studied by Plunk (2013) with the additional inclusion of finite-Larmor-radius effects.

3.1. *Case–Van Kampen energy*

The linear eigenmodes of this equation satisfy

$$(\omega - v_\parallel k_\parallel)f = k_\parallel S(v_\parallel)\int f(v'_\parallel)\mathrm{d}v'_\parallel, \tag{3.3}$$

where $\omega = \omega_r + i\gamma$ is the eigenvalue. We may also set the normalisation of the solutions to

$$\int_{-\infty}^{\infty} f(v_\parallel)\mathrm{d}v_\parallel = 1. \tag{3.4}$$

Equation (3.3) admits, depending on the choice of parameters (i.e. $k_\parallel$, ω_*, η, b and τ), a discrete set of damped and unstable modes (see Appendix A) which come in conjugate symmetric pairs (due to the time reversal symmetry of the kinetic equation without collisions) which we denote as

$$f_n = S(v_\parallel)/(\omega_n/k_\parallel - v_\parallel), \tag{3.5}$$

and a continuum of singular undamped 'Van Kampen' modes with $\gamma = 0$ which we denote as

$$f_\omega = P[S(v_\parallel)/(\omega/k_\parallel - v_\parallel)] + \lambda(\omega)\delta(\omega/k_\parallel - v_\parallel), \tag{3.6}$$

where P symbolically indicates that the Cauchy principal value should be taken upon integration. Integrating (3.3) for a discrete mode yields the linear dispersion relation

for the slab ITG mode

$$1 - \int_{-\infty}^{\infty} \frac{k_\| S(v_\|)}{\omega_n - v_\| k_\|} \mathrm{d}v_\| = 0. \tag{3.7}$$

In the case of the continuum modes, integrating (3.3) does not constitute a dispersion relation, due to the singularity at $v_\| = \omega/k_\|$, and instead sets the normalisation of the singular modes that determines $\lambda(\omega)$ (see van Kampen & Felderhof 1967)

$$\lambda(\omega) = 1 - P \int \frac{k_\| S(v_\|)}{\omega - v_\| k_\|} \mathrm{d}v_\|. \tag{3.8}$$

This system is directly analogous to the system studied by Case and Van Kampen, where it was shown by Case (1959) that this set of linear eigenmodes, comprising the discrete and continuum modes, is complete, in the sense that any distribution function $f(v_\|, t)$ can be written as

$$f(v_\|, t) = \sum_n a_n(t) f_n(v_\|) + \int A(\omega, t) f_\omega(v_\|) \, \mathrm{d}\omega. \tag{3.9}$$

The coefficients of this eigenmode decomposition can be computed by exploiting the orthogonality of eigenmodes with respect to the eigenmodes of the adjoint equation of (3.3) (given in Appendix B), which we denote as $\tilde{f}_n$ and $\tilde{f}_\omega$ for the discrete and continuum branches, respectively.

We now wish to use these features of the kinetic equation to construct an energetic norm which is 'aware' of the linear eigenmodes in which we are interested. To do this, we first project (3.1) onto the basis of discrete eigenmodes by applying

$$\frac{1}{C_n} \int_{-\infty}^{\infty} \tilde{f}_n(v_\|)(\ldots)\mathrm{d}v_\|, \tag{3.10}$$

and noting that ω_n must satisfy (3.7). This yields the simple relation

$$\frac{\partial a_n}{\partial t} = -i\omega_n a_n, \tag{3.11}$$

which implies that

$$\frac{\mathrm{d}}{\mathrm{d}t} \sum_n |a_n|^2 = 2 \sum_n \gamma_n |a_n|^2, \tag{3.12}$$

where we have summed over all the discrete modes. Equation (3.12) states that the amplitudes of the projection coefficients all grow in time according to their growth rate γ_n. Next, we turn our attention to the continuum modes. Performing the projection in a similar manner as for the discrete spectrum and recognising the normalisation condition of the Van Kampen modes gives $\partial A(\omega, t)/\partial t = -i\omega A(\omega, t)$. Because ω is purely real for these modes, we have

$$\frac{\mathrm{d}}{\mathrm{d}t} \int |A(\omega, t)|^2 \mathrm{d}\omega = 0. \tag{3.13}$$

Now by combining (3.12) and (3.13) we can construct what we will refer to as the Case–Van Kampen energy, which we define as

$$E = \sum_n |a_n(t)|^2 + \int |A(\omega, t)|^2 \mathrm{d}\omega. \tag{3.14}$$

The energy balance equation for E is now simply

$$\frac{\mathrm{d}E}{\mathrm{d}t} = 2 \sum_n \gamma_n |a_n|^2. \tag{3.15}$$

The energy E constitutes a positive definite norm of any distribution function $f(v_{\parallel})$ due to the completeness of the eigenmodes. For a given f, E grows (or damps) at a rate determined by the magnitude of its projection onto the discrete eigenmodes.

3.2. *Optimal modes and tightest possible bounds*

The Case–Van Kampen energy is a natural choice as a norm for bounding the growth of linear instabilities as it is simply a sum of eigenmode amplitudes, thus it exhibits no 'non-normal' or 'transient growth' in the absence of linear instability (i.e. it is explicitly aware that the Van Kampen modes cannot sustain linear growth, whereas other norms may be made to grow transiently by a superposition of these modes). While such transient growth is important for understanding nonlinear instability growth e.g. in scenarios where subcritical turbulence is of interest (Krommes 1997; Barnes *et al*. 2011; Landreman, Plunk & Dorland 2015; van Wyk *et al*. 2016), it seems relatively unimportant in scenarios in which the relevant parameters are well above the linear instability threshold where robustly growing instabilities can be expected.

We can now derive the optimal modes of E by writing the energy balance (3.15) as $\mathrm{d}E/\mathrm{d}t = 2K$ and defining the instantaneous growth rate of E as $\Lambda \equiv K/E$. The optimal modes are the solutions f which extremise Λ, and can be constructed by writing $E \equiv (f, \mathcal{E}f)$, and $K \equiv (f, \mathcal{K}f)$ with the familiar inner product

$$(f_1, f_2) = \int \frac{f_1^* f_2}{\bar{F}_0} \mathrm{d}v_{\parallel}. \tag{3.16}$$

The optimal modes then satisfy the generalised eigenvalue problem

$$\Lambda \, \mathcal{E} \, f = \mathcal{K} \, f, \tag{3.17}$$

where the operators $\mathcal{E}$ and $\mathcal{K}$ are given in Appendix B. To solve the optimal mode problem, we now consider the projection of (3.17) with a discrete eigenmode of the linear problem f_m with the inner product $\Lambda(f_m, \mathcal{E}f) = (f_m, \mathcal{K}f)$. Due to the orthogonality of the eigenmodes with the adjoint eigenmodes, we find (see Appendix B)

$$\Lambda = \gamma_m. \tag{3.18}$$

Similarly, considering the projection with a continuum mode, $\Lambda(f_\omega, \mathcal{E}f) = (f_\omega, \mathcal{K}f)$, yields $\Lambda = 0$. Thus there is a one-to-one correspondence between the linear growth spectrum and the optimal Λ solutions. Moreover, the optimal modes maximising $E^{-1}\mathrm{d}E/\mathrm{d}t$ are exactly the linear eigenmodes.

This may feel like a somewhat trivial consequence of the diagonalisation of the linear operator by the linear eigenmodes, but there are several takeaways from this result. Firstly, the growth of linear eigenmodes can be bounded with arbitrary tightness by the optimal modes of an energetic norm, with the tightest possible bound (i.e. equality of (1.1)) being given by the Case–Van Kampen energy. We note that this tightest bound may not be given uniquely by this energy norm. For instance, E can be defined with arbitrary weights on each of the amplitude coefficients.

Secondly, any kinetic system for which the Case–Van Kampen energy is a nonlinear invariant is nonlinearly stable if it is linearly stable because Λ will be identically zero for all $k_\perp$, i.e. subcritical turbulence is impossible. An example of such a system is the two-dimensional drift-kinetic toroidal ITG discussed by Plunk (2015). Moreover, as presented in DelSole (2004), Landreman *et al.* (2015) and Plunk & Helander (2022), for statistically steady turbulence to exist in these systems where E is a nonlinear invariant when summed over all wavenumbers, it must be the case that $\sum_k \langle \mathrm{d}E_k/\mathrm{d}t \rangle = 0$, where $\langle \ldots \rangle$ denotes a time average over the turbulent time scale, and the index k has been added. In this case $\sum_{n,k} \gamma_{n,k} \langle |a_{n,k}|^2 \rangle = 0$, such that, in the turbulent phase, the distribution function must project equally on to growing and damped eigenmodes on average.

4. Constrained optimal modes

We have demonstrated that linear instability growth may be bounded with arbitrary tightness by the instantaneous optimals of an energetic norm. However, these tightest bounds require complete knowledge of the linear spectrum. In this section, we demonstrate that we can construct energetic bounds that have the same qualitative dependence on key parameters as the linear growth rate by including only some features of the linear eigenmodes in the analysis. This avoids the requirement of prior knowledge of the solution to the linear problem.

A key feature of the linear eigenmodes, which has been absent from the optimal mode analyses involving simple energetic norms, is the real frequency ω_r. This oscillation frequency determines the relative phases of the different degrees of freedom of the eigenmode (e.g. the various fluid moments) and is associated with some of the stabilising 'resonant' effects that are not captured by the instantaneous upper bounds, which do not have an associated real frequency. As such, the optimal modes considered thus far, with the exception of the Case–Van Kampen optimals discussed in the previous section, are largely unconstrained in the allowable phase relations between their different degrees of freedom.

Here, we seek a means to include phase information into the optimal mode analysis of a simple, positive definite energy norm – the Helmholtz free energy (Helander & Plunk 2022). For the reduced-dimensionality kinetic equation (2.3), the Helmholtz free-energy balance is

$$\frac{\mathrm{d}H}{\mathrm{d}t} = 2D, \tag{4.1}$$

where

$$H = T_i \int \frac{|\bar{g}|^2}{\bar{F}_0} \mathrm{d}v_\parallel - \frac{e^2 n}{T_i}(1 + \tau)G_{\perp 0}|\phi|^2, \tag{4.2}$$

and

$$D = \mathrm{Re}\left\{ i\omega_* \eta \, G_{\perp 0} e\phi \int \bar{g}^* x_\parallel^2 \, \mathrm{d}v_\parallel \right\}. \tag{4.3}$$

To include the frequency information, we constrain the optimal mode analysis, such that the allowed distribution functions are those that share some key features with the linear modes. Thus, we seek distribution functions that maximise dH/dt subject to a set of constraint equations that are also satisfied by the linear eigenmodes.

Because the free-energy extraction D depends only on two 'fluid' moments of $\bar{g}$, natural choices for these constraints are the linear moment equations. To keep the analysis relatively simple, we consider only the two lowest-order moments as constraints. We denote these moments of $\bar{g}$ by

$$\kappa_1 = \frac{1}{n} \int \bar{g} dv_{\parallel}, \tag{4.4}$$

$$\kappa_2 = \frac{1}{n} \int \left(\frac{v_{\parallel}}{v_T} \right) \bar{g} \, dv_{\parallel}, \tag{4.5}$$

$$\kappa_3 = \frac{1}{n} \int \left(\frac{v_{\parallel}^2}{v_T^2} \right) \bar{g} \, dv_{\parallel}. \tag{4.6}$$

The moment equations for the density, κ_1, and the parallel flow, κ_2, obtained by taking the respective moments of (2.3), are given by

$$\frac{\partial \kappa_1}{\partial t} + i v_T k_{\parallel} \kappa_2 = \frac{1}{1+\tau} \left[G_{\perp 0} \left(\frac{\partial}{\partial t} + i \omega_*(1 - \eta) \right) + i \omega_* \eta G_{\perp 2} \right] \kappa_1, \tag{4.7}$$

and

$$\frac{\partial \kappa_2}{\partial t} + i v_T k_{\parallel} \kappa_3 = 0. \tag{4.8}$$

We now require that these moments evolve in time like linear eigenmodes (i.e. they satisfy the same phase relation as the moments of a linear eigenmode), such that $\partial \kappa_{1,2}/\partial t = -i\omega' \kappa_{1,2}$, where $\omega' = \omega'_r + i\gamma'$. The linear moment equations then become

$$\alpha \kappa_1 - v_T k_{\parallel} \kappa_2 = 0, \tag{4.9}$$

and

$$\omega' \kappa_2 - v_T k_{\parallel} \kappa_3 = 0, \tag{4.10}$$

where we have defined

$$\alpha = \omega' - \frac{1}{1+\tau} (G_{\perp 0} \left[\omega' - \omega_*(1 - \eta) \right] - \omega_* \eta \, G_{\perp 2}). \tag{4.11}$$

In addition to these phase relations between moments, linear eigenmodes have the property that free energy increases at exactly twice the growth rate of the mode, which can be expressed in terms of the free-energy balance (4.1) as an additional constraint

$$D = \gamma' H. \tag{4.12}$$

The distribution functions that satisfy (4.9), (4.10) and (4.12) make up a subspace of the larger space of all possible $\bar{g}$ and, importantly, the linear eigenmodes are themselves included in that subspace. In other words, ω' need not be an eigenvalue of (2.3), but the true eigenmodes also satisfy (4.9), (4.10) and (4.12) with $\omega' \to \omega$.

Therefore, distribution functions which extremise free-energy growth, while satisfying the constraints (4.9), (4.10) and (4.12) place a rigorous upper bound on the growth rate of true eigenmodes. To state this problem formally, we consider the Lagrangian

$$L \equiv D - \Lambda(H - H_0) - \lambda_1(\gamma' H - D)$$
$$- \lambda_2^*(\alpha^* \kappa_1^* - v_T k_\parallel \kappa_2^*) - \lambda_2(\alpha \kappa_1 - v_T k_\parallel \kappa_2)$$
$$- \lambda_3^*(\omega'^* \kappa_2^* - v_T k_\parallel \kappa_3^*) - \lambda_3(\omega' \kappa_2 - v_T k_\parallel \kappa_3). \quad (4.13)$$

Here, to extremise L is to extremise the free-energy drive D, subject to several constraints, which are enforced by Lagrange multipliers denoted by Λ (which will become the optimal growth) and λ_n. Here, Λ keeps the free energy fixed to some normalising value H_0, the complex multipliers λ_2 and λ_3 enforce the moment constraints and λ_1 ensures that the value of γ' from these moment constraints is consistent with free-energy balance. Each of these constraints are enforced at the extrema of L, as is evident from taking $\delta L/\delta \Lambda = 0$ and $\delta L/\delta \lambda_n = 0$.

Computing the optimal modes via $\delta L/\delta \bar{g} = 0$ and making use of the inner product

$$(\bar{g}_1, \bar{g}_2) = T_i \int \frac{\bar{g}_1^* \bar{g}_2}{\bar{F}_0} \mathrm{d}v_\parallel, \quad (4.14)$$

we arrive at the following kinetic problem for the optimal $\bar{g}$

$$(\Lambda - \gamma' \lambda_1) \left(\bar{g} - \frac{\bar{F}_0 G_{\perp 0}}{(1+\tau)} \kappa_1 \right) = (1 - \lambda_1) \frac{i \omega_* \eta \bar{F}_0 G_{\perp 0}}{2(1+\tau)} \left(x_\parallel^2 \kappa_1 - \kappa_3 \right)$$
$$- \frac{\lambda_2^* \bar{F}_0}{n T_i} \left(\alpha^* - x_\parallel v_T k_\parallel \right) - \frac{\lambda_3^* \bar{F}_0}{n T_i} \left(\omega'^* x_\parallel - x_\parallel^2 v_T k_\parallel \right). \quad (4.15)$$

This problem must be solved subject to constraint (4.9), (4.10) and (4.12).

Upon enforcing the constraint $\gamma' H = D$ in the above expression, we find the expected result that $\Lambda = \gamma'$, such that the Lagrange multiplier once again has the physical interpretation of the linear growth rate. We see that after enforcing this, the λ_1 Lagrange multiplier is arbitrary (as long as it is non-zero and not unity) such that it amounts to a renormalisation of the other multipliers. The remaining unknowns can be eliminated by noting that the system is closed by projecting onto the κ_n moments. The system of moment equations which results from this projection is given in Appendix C. After reducing the system of equations, we arrive at a quintic polynomial for $\tilde{\Lambda} = \Lambda/(\omega_* \eta)$, for which $\tilde{\Lambda} = 0$ is a solution (corresponding to the null-space of D). The remaining solutions are given by the quartic equation

$$P \tilde{\Lambda}^4 + Q \tilde{\Lambda}^2 + R = 0, \quad (4.16)$$

where the coefficients P, Q and R are given in Appendix D. We note that only solutions to (4.16) that yield a real value of Λ are valid. Complex solutions, which

are inconsistent with (4.12), are discarded. Solving this equation yields and optimal mode growth rate Λ, with an explicit dependence on the parameter ω_r'. The upper bound on linear growth is given by

$$\Lambda_{\max} \equiv \max_{\omega_r'} \Lambda. \tag{4.17}$$

The maximising value of ω_r' can, in principle, be found analytically. However, it is generally more convenient to evaluate numerically or with a computer algebra program such as Mathematica. The largest real solution to (4.16) at the optimal ω_r' gives a rigorous upper bound on the growth of the unstable eigenmodes of the slab ITG system. The bound is guaranteed to be at least as good as the unconstrained bound given by Helmholtz free-energy balance and the constraints serve to tighten this bound to the linear growth rate. Although the gyrofluid moment equations are an incomplete description of the linear eigenmodes, especially in the resonant limit, we emphasise that they are always valid constraints because they are always satisfied by the linear eigenmodes regardless of the specific parameters. While we have only considered the lowest-order moments here, the bound could be further tightened by considering a larger number of constraints, capturing more features of the linear modes.

4.1. *Features of the constrained bound*

To gain insight into the behaviour of the solutions of (4.16), we now consider some simple limits and explore the general features of the constrained optimal mode growth.

4.1.1. *Resonant stabilisation*
Firstly, to facilitate comparison with the results of Plunk & Helander (2023) we consider the long-wavelength limit where $b \to 0$ and consider a scenario without a density gradient where $\eta \to \infty$. In this limit, we have $G_{\perp 0,2} \to 1$.

In figure 1, we show the behaviour of the upper bound alongside the solution of the linear dispersion relation as a function of the instability parameter $\kappa_\parallel = \omega_* \eta / (v_T k_\parallel)$. As one would expect, the bound agrees well with the linear growth rates for large $\kappa_\parallel$, where the linear eigenmodes become more fluid-like as the lowest moments dominate the fluid hierarchy. In contrast to previous bounds (Plunk & Helander 2023), the constrained bound for the slab ITG exhibits a maximum growth rate at a finite $\kappa_\parallel$, as is the case for linear eigenmodes. This also in contrast to the simple non-resonant dispersion relation for the slab ITG mode shown in figure 1, which actually diverges in this limit (Plunk *et al.* 2014)

$$\frac{\gamma}{\omega_* \eta} = (2\tau \kappa_\parallel)^{-\frac{1}{3}}. \tag{4.18}$$

Remarkably, the constrained bound also exhibits a critical gradient, a value of $\kappa_\parallel$ below which only $\Lambda = 0$ is a valid solution. The criterion for this critical value of $\kappa_\parallel$ can be found by setting $R = 0$, such that $\Lambda = 0$ is a repeated root of (4.16) and seeking the lowest positive value of $\kappa_\parallel$ for which this can occur. In this limit, we have $\kappa_{\parallel,\mathrm{cr}} = \sqrt{2\tau(1+\tau)}$, which is precisely the critical gradient which can be derived from the linear slab ITG dispersion relation (Kadomtsev & Pogutse 1970; Plunk *et al.* 2014). Indeed, we see agreement between the critical gradient of the linear eigenmode and the bound in figure 1. This agreement in the 'resonant' limit of low-$\kappa_\parallel$ is notable given that the most unstable linear eigenmode becomes increasingly
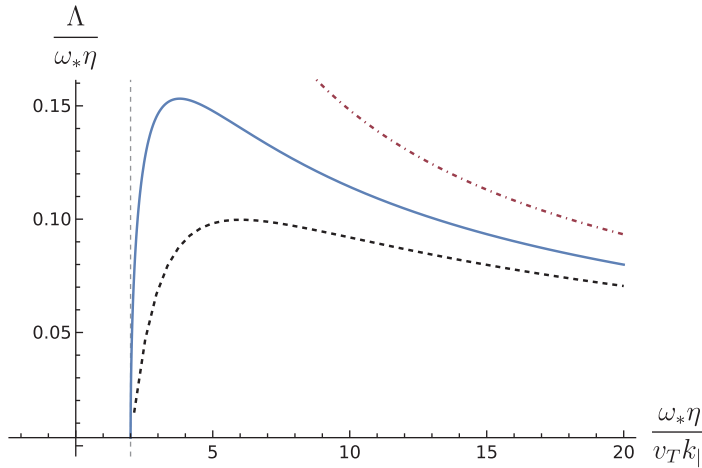
FIGURE 1. Upper bound on linear growth (blue) alongside the linear growth rate (dashed black) from the linear dispersion relation (A.1), plotted as a function of the instability parameter $\kappa_\parallel$ in the low-$k_\perp$ limit with $\eta \to \infty$ and $\tau = 1$. Also shown is the fluid-limit dispersion relation (dot-dashed red) (Plunk *et al.* 2014), which diverges as $\kappa_\parallel \to 0$. The vertical light-grey dashed line is the critical gradient of Kadomtsev & Pogutse (1970).

singular as the critical $\kappa_\parallel$ is approached. As a result, one might not expect to capture this behaviour with a finite-dimensional system of moment equations. On the other hand, the critical gradient expression derived by Kadomtsev & Pogutse (1970), which amounts to solving a two-dimensional system of equations, gives some indication that the resonant stabilisation of the slab ITG is not as complicated as one may expect and can be captured with relatively few degrees of freedom. The constrained optimal modes are, evidently, successful in capturing this resonant stabilisation due to the inclusion of information about the real frequency via ω_r', which is responsible for the effect in the linear dispersion relation.

4.1.2. Density gradient stabilisation

We now consider a finite value of η, such that the density gradient is non-zero. This is known to have a significant stabilising effect on linear ITG instabilities. The previous, nonlinear bounds of Helander & Plunk (2022) and Plunk & Helander (2023) do not capture this effect because the adiabaticity of the electrons precludes the density gradient from being a source of free energy. In figure 2, we show that the constrained optimal growth rate has the same qualitative dependence on η as the linear instability growth. Once again, we see that the critical value of η agrees with that of the linear dispersion relation. In the linear theory, this stabilisation by the density gradient is connected with the real frequency of the ITG, hence why the constrained upper bound captures this effect.

4.1.3. Finite-Larmor-radius effects

Finally, we consider how the upper bound from the constrained optimal modes depends on the normalised perpendicular wavenumber $k_\perp \rho$. In the case of the slab ITG, because the resonance does not involve the perpendicular velocity, the finite-Larmor-radius (FLR) effects manifest via the velocity-space-independent functions $G_{\perp 1,2}$. As a result, the most consequential step for capturing the FLR dependence
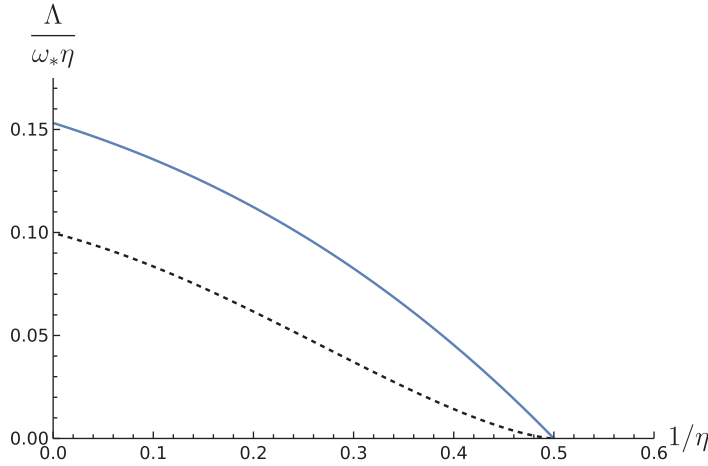
FIGURE 2. Upper bound on linear growth (blue) alongside the linear growth rate (dashed black) from the linear dispersion relation (A.1), plotted as a function of $1/\eta$ in the low-$k_\perp$ limit with $\tau = 1$. Here, both the upper bound and the linear growth rate have been maximised over $k_\parallel$.
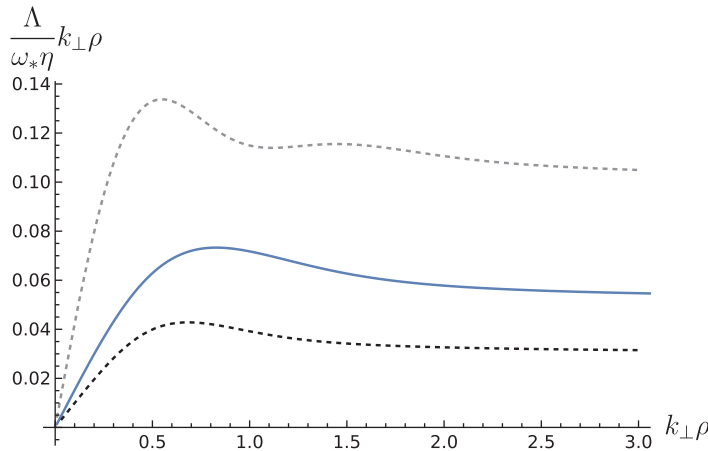

FIGURE 3. Upper bound on linear growth (blue) alongside the linear growth rate (dashed black) from the linear dispersion relation (A.1) and the nonlinear bound of Helander & Plunk (2022) and Plunk & Helander (2023) (dashed grey), plotted as a function of $k_\perp\rho$ in the limit of $\eta \to \infty$ for $\tau = 1$, where both the constrained upper bound and the linear growth rate have been maximised over $k_\parallel$.

of the slab ITG is the integration over the $v_\perp$ coordinate when going from (2.1) to (2.3). In figure 3, we see that the constrained optimal growth has a very similar qualitative dependence on $k_\perp\rho$ to the linear growth rate, and is significantly lower than the pervious bound of Plunk & Helander (2023).

5. Conclusions

Two pieces of theoretical progress towards tighter energetic bounds on linear insta-bilities have been made in this work. The first is the development of the Case–Van

Kampen energy, which provides proof that linear energetic bounds can be made arbitrarily tight to the growth rate of linear eigenmodes. This special energy is of largely theoretical interest, requiring complete knowledge of the linear eigenspectrum to construct. Nevertheless, it provides a solid foundation for the endeavour of tightening linear bounds, as well as some indication of how such tighter bounds can be constructed, namely by including information from the linear spectrum. It remains to be seen if such an energy can be constructed in non-trivial magnetic geometry.

The second theoretical development made here was to consider the constrained optimal modes. These modes extremise the growth of the Helmholtz free energy subject to linear moment constraints and capture the key parametric dependencies of the linear growth rate. They are derived from a simple, thermodynamic energy norm without requiring an explicit solution to the linear problem, in keeping with the spirit of the original nonlinear bounds of Helander and Plunk. To compute the upper bound from these modes in the slab ITG limit requires solving a simple polynomial and optimising over a free parameter ω'_r, much like the generalised free-energy bounds (Plunk & Helander [2023](); Costello & Plunk [2025]()). The inclusion of this real frequency in the optimal mode analysis introduces some key 'resonant' features of the linear slab ITG; a critical gradient below which eigenmode growth is impossible, and density gradient stabilisation. The constrained optimals are similar to work by Kotschenreuther *et al.* [(2024)](), where free-energy growth of linear modes is dynamically constrained.

The constrained optimal mode theory developed here warrants comparison with traditional linear gyrofluid theory, wherein the infinite hierarchy of fluid moments (discussed in terms of a projection onto a Hermite–Laguerre basis in more modern work) is truncated to give an approximation of the linear eigenvalue problem. Such theories involve choosing a closure in the truncation of the moment system. This closure can be chosen in a myriad of ways but is often selected to capture resonant effects that are beyond the typical regimes of validity of a truncation based on the smallness of higher-order moments due to some asymptotic argument, e.g. collisional (Braginskii [1965]()) or strongly driven closures (Plunk *et al.* [2014]()). An optimal choice for the closure model is an open, and active, research problem, with proposed closures ranging from ad-hoc (but effective) closures (Hammett & Perkins [1990]()) to recently developed machine learning approaches (Huang, Dong & Wang [2025](); Barbour *et al.* [2025]()). In contrast, the constrained optimal modes capture the qualitative behaviour of the linear growth rate in the resonant limit despite consisting of only a few low-order moments of the distribution function, which close as a natural consequence of the variational form of the problem. Thus, the upper bound is equally valid (but not necessary as close to the linear growth rate) at all plasma parameters.

We note that the constrained optimal modes considered here were only constrained by two fluid moments equations but, in principle, any number can be included, for instance by projection onto the Hermite–Laguerre basis (see Mandell, Dorland & Landreman [(2018)]() for details). The infinite set of linear constraints that would result from this projection would yield a constrained optimal mode with $\Lambda = \gamma_{\max}$ where $\gamma_{\max}$ is the largest linear growth rate because the optimisation subspace would be exactly the set of linear eigenmodes, which are the only distribution functions that simultaneously satisfy the infinite hierarchy of constraints. Thus, one would expect a bound that may be made progressively tighter to the linear eigenmode growth rate by adding more of these fluid constraints, although it is

unclear how rapidly such a bound would converge to the true linear growth rate. This observation could form the basis of a numerical implementation of constrained optimal modes with an arbitrary number of fluid constraints, similar to the recently developed pseudo-spectral gyrokinetic codes (Frei *et al.* 2023; Mandell *et al.* 2024).

The success of the constrained optimal modes in giving a computationally efficient upper bound of linear eigenmode growth warrants further investigation. Namely, this calculation should be extended to treat general magnetic geometry. In an arbitrary magnetic geometry, the gyrofluid constraint equatons will be differential along the magnetic field line, resulting in a system of ordinary differential equations to be solved for the upper bound. In addition to this, crucially, the gyrokinetic equation in general geometry cannot be integrated over a specific ignorable coordinate in velocity space (as was done for $v_\perp$ here) due to the dependence of the curvature and ∇B drifts on both $v_\perp$ and $v_\parallel$. In this scenario the system has more degrees of freedom, thus it remains to be seen how one should choose the set of constraint equations. If the performance of these bounds in the slab geometry are in fact indicative of their performance in more general scenarios, they could be a powerful tool for applications like stellarator optimisation. The manifestation of a critical ITG is of particular interest, as optimisation schemes based on this principle have been demonstrated to be effective (Roberg-Clark *et al.* 2023).

Acknowledgements

Funding

Declaration of interests

The authors report no conflict of interest.

Appendix A. Linear dispersion relation

The dispersion relation for the discrete eigenmodes of (3.17) is given by

$$1 + \tau + G_{\perp 0}\left(\xi Z(\xi) + \kappa_\parallel\left[\left(\frac{3}{2} - \frac{1}{\eta}\right)Z(\xi) - \xi(1 + \xi Z(\xi))\right]\right) - \kappa_\parallel G_{\perp 2} Z(\xi) = 0, \tag{A.1}$$

where $\xi = \omega/(v_T k_\parallel)$ and Z is the plasma dispersion function

$$Z(\xi) = \frac{1}{\sqrt{\pi}} \int_{-\infty}^{\infty} \frac{e^{-t^2}}{t - \xi} \mathrm{d}t, \tag{A.2}$$

which is defined for $\text{Im}(\xi) > 0$. The roots of (A.1) can be found numerically.

Appendix B. Details for § 3

B.1. *Adjoint equation*

The adjoint of (3.3) can be found by computing the adjoint of the linear operator associated with (3.3) under the L^2-inner product in $v_\parallel$, and is given by

$$(\omega - v_\parallel k_\parallel)\tilde{f} = k_\parallel \int S(v'_\parallel)\tilde{f}(v'_\parallel)\mathrm{d}v'_\parallel. \tag{B.1}$$

The eigenmodes of the adjoint problem we denote as $\tilde{f}_\omega$ for the continuum branch and $\tilde{f}_n$ for the discrete branch. For the discrete spectrum, the adjoint modes have velocity-space dependence $\tilde{f}_n = 1/(\omega_n/k_\parallel - v_\parallel)$ and the continuum modes are of the form $\tilde{f}_\omega = P[1/(\omega/k_\parallel - v_\parallel)] + \tilde{\lambda}(\omega)\delta(\omega/k_\parallel - v_\parallel)$, which satisfy the normalisation $\tilde{\lambda}(\omega) = \lambda(\omega)/S(\omega/k_\parallel)$. As shown in Case (1959), the eigenmodes of (3.3) and the adjoint problem satisfy the orthogonality relations

$$\int_{-\infty}^{\infty} \tilde{f}_n(v_\parallel)f_m(v_\parallel)\,\mathrm{d}v_\parallel = \delta_{nm}C_n, \tag{B.2}$$

and

$$\int_{-\infty}^{\infty} \tilde{f}_{\omega'}(v_\parallel)f_\omega(v_\parallel)\,\mathrm{d}v_\parallel = \delta(\omega - \omega')C_\omega, \tag{B.3}$$

for the discrete and continuum branches, respectively.

B.2. *Case–Van Kampen optimal modes*

The operators which appear in the optimal mode (3.17) are given by

$$\mathcal{E}\,f = \bar{F}_0 \left(\sum_n \frac{\tilde{f}_n^*}{|C_n|^2} \int \tilde{f}'_n f'\,\mathrm{d}\,v'_\parallel + \int \mathrm{d}\omega \frac{\tilde{f}_\omega^*}{|C_\omega|^2} \int \tilde{f}'_\omega f'\,\mathrm{d}\,v'_\parallel \right), \tag{B.4}$$

and

$$\mathcal{K}\,f = \bar{F}_0 \sum_n \gamma_n \frac{\tilde{f}_n^*}{|C_n|^2} \int \tilde{f}'_n f'\,\mathrm{d}\,v'_\parallel. \tag{B.5}$$

The projection of (3.17) with a discrete eigenmode f_m and noting the orthogonality of the eigenmodes with respect to the adjoint eigenmodes yields

$$\Lambda \sum_n \frac{\delta_{n,m}C_m^*}{|C_n|^2} \int \tilde{f}'_n f'\mathrm{d}v'_\parallel = \sum_n \gamma_n \frac{\delta_{n,m}C_m^*}{|C_n|^2} \int \tilde{f}'_n f'\mathrm{d}v'_\parallel, \tag{B.6}$$

giving $\Lambda = \gamma_m$. Projecting with a mode from the continuum annihilates the right-hand side of (3.17) by orthogonality with all the discrete modes, yielding $\Lambda = 0$.

Appendix C. System of moment equations

By noting the following integrals:

$$\frac{1}{n} \int \bar{F}_0 \mathrm{d}v_\parallel = 1, \tag{C.1}$$

$$\frac{1}{n} \int \left(\frac{v_\parallel^2}{v_T^2}\right) \bar{F}_0 \mathrm{d}v_\parallel = \frac{1}{2}, \tag{C.2}$$

$$\frac{1}{n} \int \left(\frac{v_\parallel^4}{v_T^4}\right) \bar{F}_0 \mathrm{d}v_\parallel = \frac{3}{4}, \tag{C.3}$$

equation (4.15) can be closed in terms of the κ_n moments. The system of equations is as follows:

$$\tilde{\Lambda} \left(1 - \frac{G_{\perp 0}}{(1+\tau)}\right) \kappa_1 = \frac{i}{2} \frac{G_{\perp 0}}{1+\tau} \left(\frac{\kappa_1}{2} - \kappa_3\right) - \tilde{\lambda}_2^* \tilde{\alpha}^* + \frac{1}{2} \tilde{\lambda}_3^* \kappa_\parallel^{-1}, \tag{C.4}$$

$$\tilde{\Lambda} \left(\kappa_3 - \frac{G_{\perp 0}}{2(1+\tau)} \kappa_1\right) = \frac{i}{2} \frac{G_{\perp 0}}{1+\tau} \left(\frac{3\kappa_1}{4} - \frac{\kappa_3}{2}\right) - \tilde{\lambda}_2^* \frac{\tilde{\alpha}^*}{2} + \frac{3}{4} \tilde{\lambda}_3^* \kappa_\parallel^{-1}, \tag{C.5}$$

$$2\tilde{\Lambda}\kappa_2 = \tilde{\lambda}_2^* \kappa_\parallel^{-1} - \tilde{\lambda}_3^* \tilde{\omega}'^*, \tag{C.6}$$

$$\tilde{\alpha}\kappa_1 - \kappa_\parallel^{-1}\kappa_2 = 0, \tag{C.7}$$

$$\tilde{\omega}'\kappa_2 - \kappa_\parallel^{-1}\kappa_3 = 0, \tag{C.8}$$

where we have repeated the constraint equations for clarity. We have defined $\kappa_\parallel = \omega_* \eta/(v_T k_\parallel)$, $\tilde{\alpha} = \alpha/(\omega_* \eta)$, $\tilde{\omega}' = \omega'/(\omega_* \eta) = \tilde{\omega}'_r + i\tilde{\gamma}'$ and $\tilde{\lambda}_{2,3} = \lambda_{2,3}/(nT_i(1-\lambda_1))$.

Appendix D. Coefficients

The coefficients of (4.16) are given by

$$P = 4\eta^2 \kappa_\parallel^4 (1 + \tau - G_{\perp 0})^2, \tag{D.1}$$

$$Q = 4\eta^2 \kappa_\parallel^2 (1 + \tau - G_{\perp 0})(2(1+\tau) - G_{\perp 0}) + 4\kappa_\parallel^4 \big((G_{\perp 0}(1-\eta) + G_{\perp 2}\eta)^2$$
$$+ 2\eta(1 + \tau - G_{\perp 0})(G_{\perp 0}(1-\eta) + G_{\perp 2}\eta)\tilde{\omega}_r + 2\eta^2(1 + \tau - G_{\perp 0})^2\tilde{\omega}_r^2\big), \tag{D.2}$$

$$R = 4\kappa_\parallel^4 \tilde{\omega}_r^2(G_{\perp 0}(1 - \eta(1 + \tilde{\omega}_r)) + \eta(G_{\perp 2} + (1+\tau)\tilde{\omega}_r))^2$$
$$+ \kappa_\parallel^2 \big(4G_{\perp 2}\eta^2(G_{\perp 2} + \tilde{\omega}_r(1+\tau)) - 4G_{\perp 0}\eta(1+\tau)\tilde{\omega}_r(\eta(2 + \tilde{\omega}_r) - 1)$$
$$+ 2G_{\perp 0}G_{\perp 2}\eta(4(\eta\tilde{\omega}_r - 1) + 5\eta) + 2G_{\perp 0}^2\big(2 + \eta(\eta(3 + 2\tilde{\omega}_r(3 + \tilde{\omega}_r)) - 5 - 4\tilde{\omega}_r)\big)\big)$$
$$+ \eta^2(1+\tau)(3(1+\tau) - 2G_{\perp 0}). \tag{D.3}$$

REFERENCES

BARBOUR, N., DORLAND, W., ABEL, I.G. & LANDREMAN, M. 2025 Machine-learning closure for Vlasov–Poisson dynamics in Fourier–Hermite space. arXiv: 2504.13313.

BARNES, M., PARRA, F.I., HIGHCOCK, E.G., SCHEKOCHIHIN, A.A., COWLEY, S.C. & ROACH, C.M. 2011 Turbulent transport in Tokamak plasmas with rotational shear. *Phys. Rev. Lett.* **106**, 175004.

BIGLARI, H., DIAMOND, P.H. & ROSENBLUTH, M.N. 1989 Toroidal ion-pressure-gradient-driven drift instabilities and transport revisited. *Phys. Fluids B: Plasma Phys.* **1**, 109–118.

BOURDELLE, C., GARBET, X., IMBEAUX, F., CASATI, A., DUBUIT, N., GUIRLET, R. & PARISOT, T. 2007 A new gyrokinetic quasilinear transport model applied to particle transport in tokamak plasmas. *Phys. Plasmas* **14**, 112501.

BRAGINSKII, S.I. 1965 Transport processes in a plasma. *Rev. Plasma Phys.* **1**, 205.

CASE, K.M. 1959 Plasma oscillations. *Ann. Phys.-NY* **7**, 349–364.

COSTELLO, P.J. & PLUNK, G.G. 2025 Energetic bounds on gyrokinetic instabilities. Part 4. Bounce-averaged electrons. *J. Plasma Phys.* **91**, E12.

DANNERT, T. & JENKO, F. 2005 Gyrokinetic simulation of collisionless trapped-electron mode turbulence. *Phys. Plasmas* **12**, 072309.

DELSOLE, T. 2004 The necessity of instantaneous optimals in stationary turbulence. *J. Atmos. Sci.* **61**, 1086–1091.

FREI, B.J., HOFFMANN, A.C.D., RICCI, P., BRUNNER, S. & TECCHIOLL, Z. 2023 Moment-based approach to the flux-tube linear gyrokinetic model. *J. Plasma Phys.* **89**, 905890414.

GIACOMIN, M., DICKINSON, D., DORLAND, W., MANDELL, N.R., BOKSHI, A., CASSON, F.J., DUDDING, H.G., KENNEDY, D., PATEL, B.S. & ROACH, C.M. 2025 A quasi-linear model of electromagnetic turbulent transport and its application to flux-driven transport predictions for STEP. *J. Plasma Phys.* **91**, E16.

HAMMETT, G.W. & PERKINS, F.W. 1990 Fluid moment models for Landau damping with application to the ion-temperature-gradient instability. *Phys. Rev. Lett.* **64**, 3019–3022.

HATCH, D.R., JENKO, F., NAVARRO, A.B., BRATANOV, V., TERRY, P.W. & PUESCHEL, M.J. 2016 Linear signatures in nonlinear gyrokinetics: interpreting turbulence with pseudospectra. *New J. Phys.* **18**, 075018.

HATCH, D.R., TERRY, P.W., JENKO, F., MERZ, F. & NEVINS, W.M. 2011 Saturation of gyrokinetic turbulence through damped eigenmodes. *Phys. Rev. Lett.* **106**, 115003.

HELANDER, P. & PLUNK, G.G. 2021 Upper bounds on gyrokinetic instabilities in magnetized plasmas. *Phys. Rev. Lett.* **127**, 155001.

HELANDER, P. & PLUNK, G.G. 2022 Energetic bounds on gyrokinetic instabilities. Part 1. Fundamentals. *J. Plasma Phys.* **88**, 905880207.

HENINGER, J.M. & MORRISON, P.J. 2018 An integral transform technique for kinetic systems with collisions. *Phys. Plasmas* **25**, 082118.

HUANG, Z., DONG, C. & WANG, L. 2025 Machine-learning heat flux closure for multi-moment fluid modeling of nonlinear Landau damping. *Proc. Natl. Acad. Sci. USA* **122**, 2503–11090.

KADOMTSEV, B.B. & POGUTSE, O.P. 1970 Turbulence in toroidal systems. In *Reviews of Plasma Physics* (ed. M.A. LEONTOVICH), pp. 249–400. Springer US.

KAMMERER, M., MERZ, F. & JENKO, F. 2008 Exceptional points in linear gyrokinetics. *Phys. Plasmas* **15**, 052102.

KOTSCHENREUTHER, M., LIU, X., MAHAJAN, S.M., HATCH, D.R. & MERLO, G. 2024 Transport barriers in magnetized plasmas- general theory with dynamical constraints. *Nucl. Fusion* **64**, 076033.

KROMMES, J.A. 1997 Submarginal profiles and turbulent transport: an exactly solvable model. *Phys. Plasmas* **4**, 1342–1356.

LANDREMAN, M., PLUNK, G.G. & DORLAND, W. 2015 Generalized universal instability: transient linear amplification and subcritical turbulence. *J. Plasma Phys.* **81**, 905810501.

MANDELL, N.R., DORLAND, W., ABEL, I., GAUR, R., KIM, P., MARTIN, M. & QIAN, T. 2024 GX: a GPU-native gyrokinetic turbulence code for tokamak and stellarator design. *J. Plasma Phys.* **90**, 905900402.

MANDELL, N.R., DORLAND, W. & LANDREMAN, M. 2018 Laguerre–Hermite pseudo-spectral velocity formulation of gyrokinetics. *J. Plasma Phys.* **84**, 905840108.

PLUNK, G.G. 2013 Landau damping in a turbulent setting. *Phys. Plasmas* **20**, 032304.

PLUNK, G.G. 2015 On the nonlinear stability of a quasi-two-dimensional drift kinetic model for ion temperature gradient turbulence. *Phys. Plasmas* **22**, 042305.

PLUNK, G.G. & HELANDER, P. 2022 Energetic bounds on gyrokinetic instabilities. Part 2. Modes of optimal growth. *J. Plasma Phys.* **88**, 905880313.

PLUNK, G.G. & HELANDER, P. 2023 Energetic bounds on gyrokinetic instabilities. Part 3. Generalized free energy. *J. Plasma Phys.* **89**, 905890419.

PLUNK, G.G., HELANDER, P., XANTHOPOULOS, P. & CONNOR, J.W. 2014 Collisionless microinstabilities in stellarators. III. The ion-temperature-gradient mode. *Phys. Plasmas* **21**, 032112.

PODAVINI, L., HELANDER, P., PLUNK, G.G., & ZOCCO, A. 2025 Energetic bounds on gyrokinetic instabilities. Part 5. Contrasting optimal and normal modes over the geometric landscape. *J. Plasma Phys.* **91**, E79.

PUESCHEL, M.J., FABER, B.J., CITRIN, J., HEGNA, C.C., TERRY, P.W. & HATCH, D.R. 2016 Stellarator turbulence: subdominant eigenmodes and quasilinear modeling. *Phys. Rev. Lett.* **116**, 085001.

ROBERG-CLARK, G.T., PLUNK, G.G., XANTHOPOULOS, P., NÜHRENBERG, C., HENNEBERG, S.A. & SMITH, H.M. 2023 Critical gradient turbulence optimization toward a compact stellarator reactor concept. *Phys. Rev. Res.* **5**, L032030.

VAN KAMPEN, N.G. & FELDERHOF, B.U. 1967 *Theoretical Methods in Plasma Physics*. North-Holland Publishing Company.

VAN WYK, F., HIGHCOCK, E.G., SCHEKOCHIHIN, A.A., ROACH, C.M., FIELD, A.R. & DORLAND, W. 2016 Transition to subcritical turbulence in a tokamak plasma. *J. Plasma Phys.* **82**, 905820609.